

UDC 629.429.3:621.313

Oleksandr Khaustov¹, Borys Liubarskyi^{2*}

¹Postgraduate student, Department of Electric Transport and Locomotive Engineering, National Technical University "Kharkiv Polytechnic Institute", 2, Kyrpychova str., Kharkiv, 61002, Ukraine. ORCID: <https://orcid.org/0009-0001-0363-6173>.

²Professor, Department of Electric Transport and Locomotive Engineering, National Technical University "Kharkiv Polytechnic Institute", 2, Kyrpychova str., Kharkiv, 61002, Ukraine. ORCID: <https://orcid.org/0000-0002-2985-7345>.

*Corresponding author: boris1911@ukr.net.

Optimization of energy storage parameters of electric buses charged at terminal stops

The paper developed a methodology for determining the optimal parameters of a combined energy storage for an electric bus based on solving a conditional minimization problem taking into account the driving mode, route parameters, and weight and size restrictions when charging the storage at the final stops of the route. The practical significance of the work lies in determining the parameters of combined energy storage for an electric bus using the example of a multi-component energy storage. Analysis of the results of the study on solving the optimization problem proved that for economical driving on routes 4 and 10, three-component storage with 1 branch with LTO cells and 28 branches with LFP cells and 1 branch of supercapacitors are optimal. For driving in intermediate and high-speed modes, two-component storage with the parameters: 2 branches with LTO cells and 15 branches with LFP cells and 1 branch with LTO cells and 47 branches with LFP cells, respectively, are optimal. For the obstacle mode, a storage device operating in the "high-speed" mode is sufficient for 10 routes, however, for the 4th route, which requires higher energy consumption, it is necessary to use a mono-component LFP - element storage device with 81 branches.

Keywords: *traction drive, energy storage, electric bus, trolleybus, parameter optimization, objective function*

Introduction. Within the urban fabric of Ukraine's major metropolitan areas, trolleybuses and their modern successors, electric buses, have established themselves as the principal modalities of trackless passenger transport, collectively constituting a substantial proportion of the municipal vehicle fleets. Their pervasive deployment, a process initiated in the latter half of the twentieth century and persistently ongoing, is fundamentally predicated upon a suite of operational advantages they exhibit over conventional internal combustion engine buses.

Foremost among these merits is their superior environmental profile; as vehicles powered by external electrification, trolleybuses generate zero direct harmful emissions at the point of use, with their environmental impact being predominantly indirect and contingent upon the generation mix of the electrical grid. A second, significant advantage lies in their capacity for kinetic energy recuperation. Through regenerative braking systems, contemporary trolleybus models can reclaim and feedback into the overhead contact wire up to 70% of the energy otherwise dissipated as heat during deceleration. Thirdly, from a lifecycle perspective, trolleybuses typically demonstrate an extended service longevity compared to buses, a characteristic attributable to the absence of high-vibration internal combustion engines, which consequently imposes reduced mechanical stress on structural components.

Notwithstanding these notable benefits, it would be an oversimplification to envisage the conventional trolleybus of future urban transit ecosystems due to a constellation of inherent operational limitations. A primary constraint is their compromised maneuverability, dictated by an absolute dependence on a fixed overhead contact network. This tethering not only restricts routing flexibility but also necessitates considerable capital investment for the initial infrastructure deployment and any subsequent network expansion. Furthermore, trolleybuses exhibit a pronounced sensitivity to both the integrity of the road surface and the condition of the contact infrastructure. Traversing degraded road sections mandates a significant reduction in velocity to prevent the dewirement of the current collection pantographs. Moreover, the intrinsic design of contact network elements—such as intersections, switches, and sectional insulators on drawbridges—imposes mandatory speed restrictions for safe passage. An additional vulnerability is their susceptibility to the icing of contact wires, a phenomenon that can severely degrade the quality of electrical contact and accelerate the abrasive wear of the pantograph's contact inserts. Finally, the perpetual maintenance demands of the extensive overhead wire system necessitate a dedicated cadre of skilled personnel, a requirement that poses acute challenges in the context of martial law in Ukraine, complicating both training and retention of such specialized staff.

The synthesis of the aforementioned advantages with the mitigation of the described disadvantages is potentially achievable through the adoption of battery electric buses, or simply electric buses, as a primary mode of public conveyance. This technology retains a high degree of environmental and energy efficiency while conferring excellent operational maneuverability, thereby enabling dynamic and flexible routing with permissible deviations. The principal limiting parameters in this context are the energy density and capacity of the onboard energy storage systems and the concomitant availability of a suitably distributed charging infrastructure.

For the purpose of a comprehensive analysis of energy consumption in trackless electric public transport, the following vehicle typologies, distinguished by their energy storage and charging strategies, are considered:

A long-range electric bus, equipped with high-capacity energy storage systems that afford an autonomous operational range of approximately 150 to 250 kilometers. This class primarily relies on scheduled charging sessions, typically conducted overnight within depot facilities.

A medium-range electric bus, featuring a battery of moderate capacity designed for an autonomy of up to 50 kilometers. Its operational paradigm is supported by frequent, fast-charging interventions (with durations of 10 to 30 minutes) at terminal stops or designated charging stations along the route.

A short-range electric bus, utilizing a minimally-sized battery pack sufficient for a range of up to 10 kilometers. This model depends on opportunistic, short-term charging sessions at regular passenger stops, with charging durations comparable to the time spent for passenger boarding and alighting.

A pivotal and actively pursued research domain within this field is the development of sophisticated energy flow management strategies for electric power conversion systems that are equipped with hybrid or combined energy storage assemblies. The conceptual advancement embodied by this technology is the systemic integration of heterogeneous storage elements—specifically, those engineered for high power density (to manage rapid charge/discharge cycles, e.g., during acceleration and regenerative braking) synergistically with those optimized for high energy density (to sustain extended range and base load).

Analysis of recent research and problem statement. An examination of hybrid energy storage systems, which integrate disparate lithium-cell chemistries, was conducted in [1]. The investigation revealed that such heterogeneous configurations yield a marked enhancement in performance metrics, demonstrating a 5.56% increase in energy density and a substantial 28.21% improvement in specific energy relative to conventional, homogeneous lithium-cell battery assemblies. Corroborating these findings, the research delineated in [2] established that hybrid topologies—specifically those synergistically combining Nickel Manganese Cobalt (NMC) cells, prized for their high specific energy, with Lithium Titanate (LTO) cells, renowned for their high specific power—can achieve a mass reduction of up to 33.5% or a cost diminution of up to 30% compared to monochemical battery systems. Further substantiating the economic viability of this approach, the optimization study presented in [3],

focused on hybrid batteries comprising lithium cells of different chemistries, concluded that such hybrid energy storage systems possess the potential to significantly reduce aggregate costs in comparison to systems utilizing a single cell type.

Consequently, scholarly inquiries dedicated to the determination of optimal parameters and the development of sophisticated methodologies for the optimization of hybrid energy storage devices for electric rolling stock are of profound contemporary relevance. These research endeavors provide a critical pathway for achieving substantial enhancements in the efficacy and performance of energy storage technologies deployed in modern vehicular assets.

When undertaking an assessment of energy efficiency, it is imperative to ensure a high degree of fidelity between calculated models and the actual operational parameters empirically recorded during the service of public transport within a dense urban milieu. To this end, the development of a representative driving cycle is a foundational prerequisite. This cycle must constitute a computationally derived velocity-time profile that accurately encapsulates the real-world kinematic patterns—comprising accelerations, decelerations, idling periods, and cruising speeds—characteristic of trackless passenger vehicles navigating city streets.

The initial phase in the derivation of such a cycle involved the selection of a prototypical urban public transport route. For this study, the selection process was predicated upon bus routes operational within the Ukrainian city of Ivano-Frankivsk, a locale characterized by high traffic density and recurrent congestion at the time of the investigation [4,5]. To identify the route most faithfully reflective of standard urban public transport operating conditions, a set of rigorous selection criteria was instituted. Primarily, the analysis was confined exclusively to bus routes, as the principal research objective was to scrutinize technical solutions for enhancing the environmental performance of the extant trackless public transport fleet via a transition to electric traction. Secondly, a stipulation was imposed that all intermediate stops along the candidate route must be situated strictly within the city's jurisdictional boundaries. Thirdly, a meticulous spatial analysis of the stop distribution was performed, with particular emphasis accorded to routes traversing the central and historical districts, which typically present the most demanding operational profiles. Based on a holistic application of these considerations, bus Routes 4 and 10 were identified as possessing the highest degree of representativeness for subsequent modeling [6,7,8].

The application of this representative cycle to the sizing of an energy storage system for electric buses on Routes 4 and 10, under a depot-charging operational paradigm [9], indicates that a single- or dual-component storage architecture is optimal. The implementation of a three-component storage device, by contrast, was determined to be non-optimal. For an economical operational mode on Route 4, the optimal configuration is a two-component accumulator, comprising 147 branches equipped with Lithium Iron Phosphate (LFP) elements and 1 branch with supercapacitors. For Route 10, a mono-accumulator based on 131 branches of LFP elements was found to be optimal. This specific operational mode is applicable when organizational requirements for electric bus deployment are coupled with rational stipulations for passenger transportation speeds. The mass of the optimal storage systems for Routes 4 and 10 is 2.52 tonnes and 2.14 tonnes, respectively, with associated costs of 115 thousand euros and 93.52 thousand euros.

However, when the operational model shifts to "with obstacles" modes—simulating scenarios of severe traffic congestion or detours—the mass and cost parameters for the storage systems on Routes 4 and 10 escalate significantly. The mass increases to 5.47 tonnes and 4.71 tonnes (representing a 2.17-fold and 2.2-fold increase), while the cost rises to 245.8 thousand euros and 210.6 thousand euros (a 2.13-fold and 2.25-fold increase), respectively. This substantial inflation is directly attributable to a 2.31-fold intensification of the energy capacity requirements for the storage devices. Furthermore, the optimal type of storage device undergoes a transition under these constrained conditions. For Route 4, the optimal configuration becomes a two-component system with 1 branch of LTO cells and 316 branches of LFP cells, while for Route 10, a mono-component system of 281 branches with LFP cells is prescribed. Under a depot-charging regime, energy capacity emerges as the paramount indicator for storage device sizing. Nonetheless, the power output of the resultant optimal energy storage systems is

found to be excessive, exceeding the minimum requirement of 180 kW by a factor of 2.05 to 3.29, which is indicative of a sub-optimal and economically irrational allocation of resources [9].

The purpose and tasks of the study. The purpose of the work is to determine the parameters of a multi-component energy storage device for an electric bus that is charged at non-terminal stops using the example of vehicles for providing trolleybus routes 4 and 10 in Ivano-Frankivsk.

Tasks of the work.

1. Determine the energy indicators (power and energy intensity) of energy storage devices that can ensure the operation of an electric bus when servicing routes.

2. Develop a methodology for determining the parameters of a multi-component energy storage device based on conditional minimization methods.

3. Determine the parameters of a multi-component energy storage device for electric buses.

Materials and methods of research. This study focuses on a detailed analysis of trolleybus routes No. 4 and No. 10. These routes were selected for in-depth study due to their significant role in the city's public transportation structure, as they provide essential and convenient mobility services to a wide range of passenger demographics. A schematic representation of the operational route and geographic distribution of route No. 4.

A preliminary analysis of route No. 4 allows us to identify several primary segments characterized by exceptionally high traffic volumes. These critical nodes include the intersection of Halytska and Dnistrovska Streets, as well as the confluence of Dnistrovska and Vasylyanok Streets, both of which experience consistently high levels of vehicular throughput. Furthermore, recurring congestion is systematically observed along Halytska Street, particularly along the section from Trolleybusna Street to the bridge structure, including the immediate approaches and exits. An additional critical point of vehicle concentration is the intersection located directly on Halytska Street, which also experiences significant traffic volume. Fundamental operational data for route No 4, covering the section from Firma "Barva" to Dnistrovska Street, are presented in summary form in Table 1 [6,7].

Table 1. Initial data for route No. 4 Barva Company - Dnistrovska Street

Indicator name	Direct direction	Reverse direction
Route length, km	10.94	9.58
Technical speed, km/ h	29	
Number of working days, days.	365	
Number of stops, units	15	14
Zero mileage, km	0.65	0.38

In parallel, a study of route No 10 reveals a separate set of key segments characterized by difficult road conditions and persistent traffic delays. These problem areas include: the section from Symonenko Street to Mykolaychuka Street; the section from Stusa Street to Ivasyuka Street; the section from Ivasyuka Street between Stusa and Ioanna Pavla II Streets; the section from Ivasyuka Street to Nezalezhnosti Street; The intersection of Ivasyuka and Volchynetskaya Streets; as well as the section of Nezavisimosti Street from Mykytynetskaya Street to Iosifa Slipoho Street. Additional traffic congestion is regularly recorded on the bridge over the river on Tisemenitskaya Street, as well as at the intersections of Tisemenitskaya Street with Dekabristov and Yunosti Streets. The road surface condition on Avtolevmashevskaya Street is also assessed as unsatisfactory due to the prevalence of potholes. The authorized end point for the U-turn maneuver on this route is the Pressmash U-turn circle. The corresponding initial data for Route No. 10, connecting Rodon Public Joint-Stock Company with Pressmash, are systematized and presented in Table 2.

Based on empirical data collected during systematic monitoring of routes No 4 and No 10 during the 2022 operating period [4, 5], a set of key performance indicators was defined for a subsequent comprehensive assessment of the rolling stock's operational efficiency.

Table 2. Initial data on route No. 10 PJSC " Rodon " – Pressmash

Indicator name	Direct direction	Reverse direction
Route length, km	9.01	7.83
Technical speed, km/ h	28	
Number of working days, days.	365	
Number of stops, units	18	16
Zero mileage, km	0.84	0.79

Using the methodological framework outlined in [6,7], average daily operational metrics for electric rolling stock on routes No 4 and No 10 in Ivano-Frankivsk were calculated and summarized in Table 3.

Table 3. Average daily performance indicators of electric rolling stock

Indicator	majestic
Route	No.4
Average number of turnovers :	10
Clarification of operating hours of trolleybuses on the route	12.91 hours.
Check-in time in the outfit	14.94 hours.
Work productivity per day	5456.64 pass.
Daily productivity in passenger kilometers	12495.706 pass · km .
Productive mileage of a trolleybus	205.2 km.
Average daily trolleybus mileage	206.23 km.
Trolleybus mileage utilization rate	0.99.
Movement interval	19.4 min.
Movement frequency	3.09 cars / hour.
Route	No. 10
Average number of turnovers	10
Clarification of operating hours of trolleybuses on the route	12.68 hours.
Check-in time in the outfit	12.73 hours.
Work productivity per day	4640.58 pass.
Daily productivity in passenger kilometers	10255.7 pass · km.
Productive mileage of a trolleybus	168.4 km.
Average daily trolleybus mileage	170.03 km.
Trolleybus mileage utilization rate	0.99.
Movement interval	19.02 min.
Movement frequency	3.15 cars /hour.

Thus, based on the results of a comprehensive study of the operating parameters of electric rolling stock on routes No 4 and No 10 in Ivano-Frankivsk, the key parameters characterizing both vehicle performance and passenger load dynamics were successfully identified and quantified for both trolleybuses and electric buses.

Determination of energy consumption during the operation of rolling stock. The operational efficacy and economic viability of electric public transport systems are contingent not merely upon the intrinsic technical specifications of the rolling stock, but also, and to a significant degree, upon their specific regimes of operation during service. Substantial conservation of energy resources can be realized through the methodological optimization of velocity profiles adopted by vehicles traversing urban thoroughfares. The critical importance of this undertaking has been further accentuated by the contemporary context of markedly escalated electricity tariffs [10]. A fundamental operational constraint arises from the fact that trams and trolleybuses are typically not outfitted with onboard

electricity metering apparatus. Consequently, vehicle operators are deprived of direct feedback, precluding them from selecting a driving strategy that minimizes energy consumption. The monitoring of aggregate energy usage occurs solely at the level of the enterprise or substation, a practice that renders the precise attribution of consumption to specific vehicles, routes, or operational phases exceedingly challenging, if not entirely unfeasible. To address this analytical gap, the present investigation employs methodologies of mathematical modeling to scrutinize patterns of electricity consumption and to formulate consequent measures for energy conservation.

Scholarly inquiry into the enhancement of electric transport efficiency through motion control is fundamentally grounded in the principles of vehicle dynamics. A more nuanced approach to these issues involves their consideration from the perspective of automated electric drives engineered for specialized technological applications. A defining characteristic of this methodological framework is the formulation of the equation of motion with reference to the wheel rim, as opposed to the motor shaft, while adopting the distance traversed as the independent variable. Given that trams and trolleybuses generally operate without multi-speed gearboxes, the gear ratio linking the motor shaft to the wheel rim remains invariant, thereby rendering the first distinction less consequential in practice. However, the second distinction is of paramount importance, as time cannot be treated as a purely independent variable; the velocity and the very nature of the motion are themselves dependent variables that fluctuate dynamically in response to real-world operational conditions, such as traffic, gradients, and mandatory stops.

The foundational relationship governing the kinematics of electric rolling stock is described by the fundamental equation of electric traction theory, which provides the deterministic basis for calculating vehicle speed [11, 12]:

The basic equation of the theory of electric traction determines the speed of electric rolling stock [11, 12]:

$$28,3 \cdot (1 + \gamma_t) \cdot \frac{dV}{dt} = \frac{F_t(V)}{g \cdot M(t)} - w_o(V) - w_d(s), \quad (1)$$

where $\gamma_t = M_i/M_t$ – inertia coefficient;

M_t – total mass of the vehicle, t ;

M_i – additional mass of rotating parts, t (for different types of rolling stock $\gamma_t = 0.1-0.2$);

V – speed, km/h;

t – travel time, s;

$F_t(V)$ – traction force of engines in accordance with the operating mode of the traction electric drive of the vehicle;

$M(t)$ – mass of the vehicle taking into account passengers; g – acceleration of gravity m/s²;

$w_o(V)$, $w_d(s)$ – specific main and additional motion resistances [11, 12].

The main specific resistance of movement determined by the dependencies for electric buses [11, 12]

$$w_o(V) = 12 + 0,004 \cdot V^2, \quad w_d(s) = 16 + 0,004V^2. \quad (2)$$

The additional specific resistance to movement consists of resistances due to slopes $i(s)$ and from curved sections of the path $iR(s)$

$$w_d(s) = i(s) + iR(s). \quad (3)$$

For the precise determination of vehicular energy expenditure, this analysis adopts the methodological framework and data pertaining to the operational modes of electric rolling stock as established in the foundational study [11].

The velocity profile of an electric bus over a representative 600-meter route segment, delineating three distinct operational regimes: "Economic," "Fast," and "Intermediate." [11] The "Economic" mode is characterized by an initial traction phase spanning 150 meters, followed by an extended coasting phase, with deceleration initiated only 10 meters prior to a complete stop. In contrast, the "Fast" mode employs continuous traction for 470 meters, transitioning to braking for the final 130 meters. The "Intermediate" mode constitutes a hybrid approach, with traction applied for 250 meters before the vehicle enters a coasting state [11]. The corresponding current consumption of the traction drive, which is active exclusively during phases requiring motive power. Analysis confirms that energy draw is minimized in the "Economic" mode. Conversely, in the "Fast" mode, current is consumed for the majority of the trajectory, with a minimum observed value of 160 A. Following the obstruction, the vehicle resumes motion in an acceleration phase, with its current consumption profile mirroring that of the initial departure [11].

A quantitative analysis of specific electricity consumption, summarized in Table 4, reveals significant disparities across the operational modes. The "Fast" mode demands 143 Wh/t-km, the "Intermediate" mode 97.5 Wh/t-km, and the "Economic" mode merely 78 Wh/t-km. This data unequivocally demonstrates the profound potential for energy conservation through the strategic modulation of driving behavior. However, a critical implementation barrier exists: drivers are operationally bound to adhere to fixed schedule commitments. The designated operational speed for the trolleybus is approximately 16 km/h, with stipulated idling durations at stops ranging from 10 to 45 seconds. Crucially, simulations indicate that even when employing the "Economic" mode with the maximum permissible idling time, an operational speed of 17.56 km/h is achievable (Table 4). This exceeds the scheduled requirement, thereby proving that energy-efficient driving does not inherently compromise timetable adherence. Despite this, empirical observation suggests a driver propensity towards the "Fast" mode, a tendency largely attributable to the absence of real-time energy consumption feedback, which focuses driver attention singularly on schedule compliance [11].

Table 4. Results of calculation of electric bus operation indicators in different driving modes

Indicator	Driving mode			
	Economical	Intermediate	Fast	With an obstacle
Electricity consumption (travel 600m), kWh	0.77 (100%)	0.96 (125%)	1.41 (191%)	1.72 (223%)
Electricity consumption (travel 1 km), kWh W_{1km}	1,283	1.6	2.35	2,286
Travel time, s	78	60	54	90
Average speed on the section, km/h.	28.1	36	40	24
Specific electricity consumption in Wh/t km	78	97.5	143	175
As a percentage of "Fast"	54.6%	68.2%	100%	122%
Operating speed, km/h (in case of parking at a stop for 45 s)	17.56	20.57	21.81	16.0

Synthesis of research findings [11,12] indicates that a systematic transition from the "Fast" to the "Economic" driving regime can yield a substantial 45.4% reduction in energy costs. Accounting for route-specific variabilities and the probabilistic occurrence of obstacles, a conservative estimate for achievable electricity savings falls within the range of 10% to 45%.

According to the results of the research, the electricity costs for traveling 1 km by electric bus in the "Economical", "Fast", "Intermediate" and "Over obstacles" driving modes (W_{1km}) were determined, which are given in Table 5.

Based on the calculations given in [1, 3], the performance of single-cell storage devices using only LTO cells, LFP cells and supercapacitors was determined . As an example, the LTO cells YINLONG 66160H 2.3v 40ah [13], LFP cells ENERpower 26650 LiFePO4 3.2V 3000mAh (10C) [14] and

supercapacitors Maxwell 3000 FARAD Capacitor were considered. Boostcap 3000f 2.7 volt BCAP3000 [15] taking into account the technical cost parameters of the elements based on information from [1,3].

$$W_n = W_{1km} \cdot L_m, \tag{4}$$

where L_m - the mileage of the vehicle using the energy storage device, which is determined according to the storage device usage mode when charging a – the mileage is equal to the total mileage in the forward and reverse directions.

The general energy consumption indicators of storage devices for electric buses are given in Table 5.

Table 5. Energy capacities of storage devices for electric buses with

Electric bus driving mode	Vehicle route	Energy capacity of the storage tank, kWh
Economical	4	52.6
Intermediate	4	65.6
Fast	4	96.4
Behind obstacles	4	117.6
Economical	10	43.2
Intermediate	10	53.8
Fast	10	79
Behind obstacles	10	96.4

The capacity of the on-board storage device must ensure the operation of electrical equipment during the operation of the traction drive and auxiliary systems.

The power at the wheels of an electric bus is determined by the resistance force according to the expression

$$P_1 = \frac{W_0 \cdot V}{3600} = \frac{(12 + 0,004 \cdot V^2) g \cdot m \cdot V}{3600}. \tag{5}$$

The storage capacity is determined taking into account the efficiency of the traction drive determined for the traction drive of the electric bus according to the dependencies shown in [20] and the efficiency of the mechanical transmission which is $\eta_m = 0.17$ [11] and taking into account additional own needs (for heated trolleybuses it is $P_d=18$ kW)

$$P_{nak} = P_1 \cdot (\eta - \eta_m) + P_d. \tag{6}$$

Results of determining the capacity of the energy storage device for operating modes are given in Table 6.

For further research, we will use elements characterized by the following technical parameters.

The number of series-connected elements is determined by

$$K_s = \frac{u_{DC}}{u_{ch}}, \tag{7}$$

where u_{DC} – is the voltage of the intermediate circuit;
 u_{ch} – is the voltage at the end of charging the element.

The resulting value N_s is rounded up.

$$x_i = \max(K_1, K_2), \quad (8)$$

where K_1 – is the number of parallel branches, determined from the condition of ensuring the required level of energy accumulation;

K_2 – the number of parallel branches, determined from the condition of ensuring the required level of storage capacity.

Table 6. Storage capacity for electric buses

Driving mode	V	w_0	W_0	P_2	η	η_m	η_{sum}	P_1	P_n
-	km/h	H/kH	H	kW				kW	kW
Economical	50	12.78	2257	113.7	0.78	0.17	0.61	186	205
Fast	56.2	12.97	2290	128.7	0.82	0.17	0.65	197	216
Intermediate	61.2	13.15	2323	142.2	0.87	0.17	0.70	203	221
Behind obstacles	61.2	13.15	2323	142.2	0.87	0.17	0.70	203	221

The number of parallel branches, determined from the condition of ensuring the required level of energy accumulation (W_n), is determined by the expression

$$K_1 = \frac{W_n}{K_s \cdot W_{cell} \cdot k_1}, \quad (9)$$

where W_{cell} – capacity of one element, expressed in kWh;

k_1 – a coefficient that takes into account the reduction in energy that an energy storage element can store when charged with a current exceeding the optimal value. According to the recommendations [3], we take it equal to 0.9. The resulting value $N1$ is rounded up.

The number of parallel branches, determined from the condition of ensuring the required level of storage capacity, is determined by the expression

$$K_2 = \frac{P_n}{K_s \cdot u_{DC} \cdot i_{c1}}, \quad (10)$$

where P_n – nominal capacity of the storage device;

u_{DC} – discharge voltage of the cell;

i_{c1} – the smaller of the charge and discharge current of the cell $i_{c1} = \min(i_1, i_2)$.

Here i_1 – permissible charging current, i_2 – permissible discharging current.

The resulting value K_2 is rounded up.

Number of elements

$$K_{cell} = x_i \cdot K_s, \quad (11)$$

Total mass of elements

$$M = K_{cell} \cdot M_{cell}, \quad (12)$$

where m_{cell} – is the mass of one element.

We will determine the volume required to accommodate the elements of the on-board storage device

$$v = K_{cell} \cdot x_{cell} \cdot y_{cell} \cdot z_{cell}, \quad (13)$$

where x_{cell} – length of the element;

y_{cell} – width of the element;

z_{cell} – height of the element.

Cost of storage elements

$$Z = K_{cell} \cdot C_{cell}. \quad (14)$$

The total capacity of the storage elements is equal to

$$W = K_{cell} \cdot W_{cell}. \quad (15)$$

General results of calculations of basic single-cell storage devices are given in [1, 2, 3].

The calculations did not take into account the volumes and masses of the cooling system components, as well as the dimensions of the battery management system.

The presented computational models explicitly omitted the volumetric, mass, and spatial contributions associated with the constituent elements of the cooling apparatus, as well as the physical dimensions of the essential battery management system.

A synthesis of comparative analyses, as documented in the referenced studies [1, 2, 3], establishes that energy storage systems predicated upon Lithium Iron Phosphate (LFP) chemistry are characterized by the most substantial mass and volumetric footprints. In direct contrast, storage systems utilizing supercapacitors demonstrate the most favorable aggregate mass characteristics, whereas configurations based on Lithium Titanate (LTO) technology necessitate the smallest installation volume. Furthermore, the lowest aggregate component cost is similarly identified for the LTO-based storage system configuration.

The total energy density realized in a single-cell-type supercapacitor storage system approximates its nominal energy density. However, a significant disparity is observed in battery-based systems: the available energy density surpasses the minimum operational requirement by a factor of approximately 5.5 for LTO cells and a substantial 14.7 for LFP cells. While the capability to recharge the energy storage system after multiple trip cycles is a favorable attribute, the pronounced underutilization of the installed energy capacity results in considerable inefficiencies, manifesting as escalated penalties in mass, volume, and capital expenditure. Among the configurations subjected to analysis, a single-cell-type system utilizing LTO chemistry provides the most advantageous total cost, whereas an LFP-based system yields the lowest specific cost per kilowatt-hour [1, 2, 3].

When subjected to a multi-criteria assessment encompassing mass, volume, total cost, and cost per kilowatt-hour, it is evident that no single-cell energy storage technology achieves a simultaneous optimization across all performance vectors. Consequently, a rationally justified engineering solution entails the implementation of a hybrid, or combined, energy storage system. Such a system is architected to synergistically amalgamate the distinct advantages inherent to the individual cell types previously considered.

The conditional optimization of the parameters for a hybrid energy storage system is formally categorized as a constrained parameter minimization problem. Informed by the foundational work of previous studies [1, 2, 3], and taking into account the inherent uncertainties associated with long-term operational and end-of-life disposal costs, the total cost of the storage system's core components was selected as the primary objective function to be minimized. This criterion provides a robust and quantifiable basis for the system's design optimization.

The objective function has the following form

$$Z = Z_{LTO} + Z_{LFP} + Z_{SC} \rightarrow \min, \quad (16)$$

where Z_{LTO} is the cost of LTO cells;
 Z_{LFP} – is the cost of LFP cells;
 Z_{SC} – is the cost of supercapacitors.

Due to the fact that the energy storage device consists of parallel branches of connected elements, it is rational to choose the number of branches of each type of storage device as parameters for the combined storage device: x_1 – number of branches with LTO elements, x_2 – number of branches with LFP elements, x_3 – number of branches with supercapacitors.

Thus, the total cost of the elements can be determined by the expression

$$Z = x_1 \cdot Z_1 + x_2 \cdot Z_2 + x_3 \cdot Z_3 \rightarrow \min, \quad (17)$$

where Z_1 - the cost of the LTO cell branch;
 Z_2 - the cost of the LFP cell branch;
 Z_3 - the cost of the supercapacitors branch.

Let us consider the constraints (conditions) imposed on the storage parameters and used in the conditional minimization problem.

Constraints in the form of equalities. This group of constraints includes constraints that establish the required nominal power (P_n) and nominal energy capacity of the storage device (W_n)

$$P = P_{LTO} + P_{LFP} + P_{SC} = P_n, \quad (18)$$

where P_{LTO} – is the nominal power of LTO cells;
 P_{LFP} – is the nominal power of LFP cells;
 P_{SC} – is the nominal power of supercapacitors.

$$W = W_{LTO} + W_{LFP} + W_{SC} = W_n, \quad (19)$$

where W_{LTO} – is the operating energy capacity of LTO cells;
 W_{LFP} – is the operating energy capacity of LFP cells;
 W_{SC} – is the operating energy capacity of supercapacitors.

According to the approaches [16-20], to set the constraints in the minimization problem in the form of equalities, we transform them into inequalities in the form

$$P \geq P_n, \quad (20)$$

where P_n – the specified storage capacity.

$$W \geq W_n, \quad (21)$$

where W_n – the specified energy capacity of the storage device.

Taking into account the parameters of the storage device, we transform the dependencies (18)-(21) to the form necessary for solving the problem

$$x_1 \cdot P_1 + x_2 \cdot P_2 + x_3 \cdot P_3 \geq P_n, \quad (22)$$

where P_1 – is the power of branches with LTO elements;
 P_2 – is the power of branches with LFP elements;

P_3 – is the power of branches with supercapacitors.

$$x_1 \cdot W_1 + x_2 \cdot W_2 + x_3 \cdot W_3 \leq W_n, \quad (23)$$

where W_1 – is the energy density of branches with LTO cells;

W_2 – is the energy density of branches with LFP cells;

W_3 – is the energy density of branches with supercapacitors.

Let's consider restrictions in the form of inequalities. This group includes restrictions that are set for the storage device according to mass-dimensional indicators (m_n maximum mass of storage device elements, V_n maximum volume of storage device elements), i.e.

$$M = M_{LTO} + M_{LFP} + M_{SC} \leq M_n, \quad (24)$$

where M_{LTO} – is the mass of LTO cells;

M_{LFP} – is the mass of LFP cells;

M_{SC} – is the mass of supercapacitors.

$$v = v_{LTO} + v_{LFP} + v_{SC} \leq v_n, \quad (25)$$

where v_{LTO} – is the volume of LTO cells;

v_{LFP} – is the volume of energy capacity of LFP cells;

v_{SC} – is the volume of supercapacitors.

Taking into account the parameters of the components of the combined storage device, we transform the dependencies (24), (25) to the form necessary for solving the problem

$$x_1 \cdot M_1 + x_2 \cdot M_2 + x_3 \cdot M_3 \leq M_n, \quad (26)$$

where is M_1 – the mass of the LTO cell branch;

M_2 – is the mass of the LFP cell branch;

M_3 – is the mass of the supercapacitors branch.

$$x_1 \cdot v_1 + x_2 \cdot v_2 + x_3 \cdot v_3 \leq v_n, \quad (27)$$

where v_1 - the volume of the LTO-element branch;

v_2 - the volume of the LFP-element branch;

v_3 - the volume of the supercapacitors branch.

In addition to constraints in the form of equalities and inequalities according to the approaches [10-12], we set constraints on the parameters of the optimization problem

$$\begin{cases} x_{1min} \leq x_1 \leq x_{1max}; \\ x_{2min} \leq x_2 \leq x_{2max}; \\ x_{3min} \leq x_3 \leq x_{3max}, \end{cases} \quad (28)$$

where x_{1min} – the minimum number of branches of LTO elements;

x_{1max} – the maximum number of branches of LTO elements;

x_{2min} – the minimum number of branches of LFP elements,

x_{2max} – the maximum number of branches of LFP elements;

x_{3min} – the minimum number of branches of supercapacitors;

x_{3max} – the maximum number of branches of supercapacitors.

To address the formulated conditional minimization problem, the computational procedures were executed within the MATLAB software environment (developed in the United States), utilizing the specialized OptLab optimization toolkit (developed in Ukraine). This specific software combination was selected for its capacity to provide access to an extensive suite of algorithmic methods suitable for the problem class at hand. Following preliminary trials with a constrained set of test solutions, it was determined that the most efficacious results were yielded through the application of the Weyl method, particularly when initiated from a variety of distinct initial search points within the solution space.

The present study is therefore dedicated to resolving the optimization problem of identifying optimal configurations for combined (hybrid) energy storage systems across a spectrum of requisite energy and power capacities. These capacity requirements are not fixed but are dynamically determined by a complex set of operational variables. These include specific vehicle driving modes, the topographical profile and spatial trajectory of the route, and the loading parameters of the rolling stock. The foundational data and operational constraints for these plug-in hybrid power plants for electric buses are derived from the established research presented in works [1,2,3].

The complete iterative process and trajectory for solving these configuration optimization problems for the combined energy storage system are documented in detail in Fig 1-4. The graphical representations therein illustrate the solution paths, wherein the initial starting point for the optimization algorithm is explicitly marked by a circular dot, and the final, converged optimal solution is indicated by a rhombus symbol.

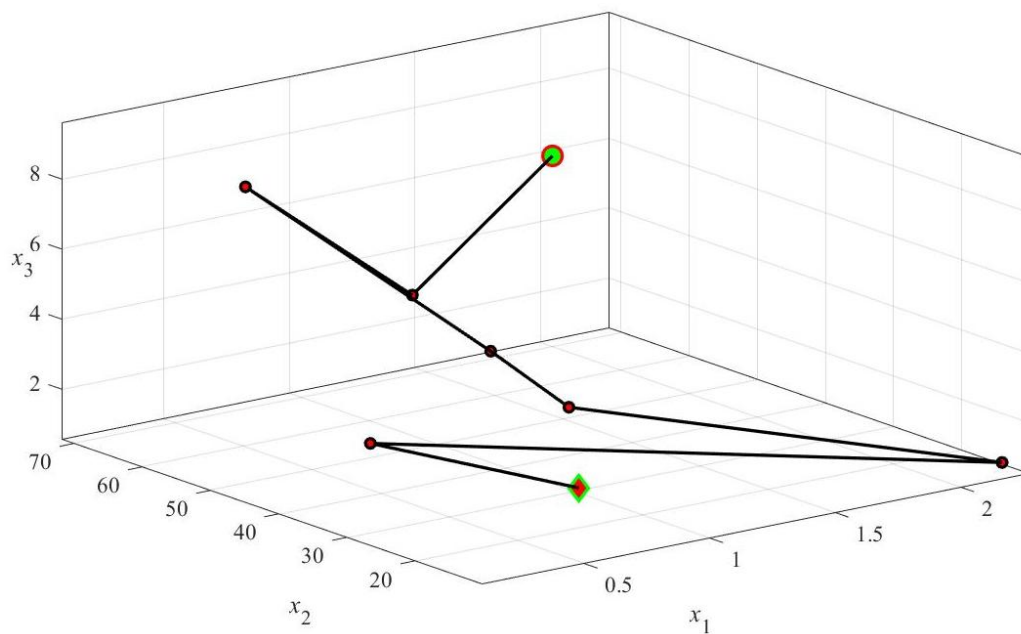


Fig. 1. The progress of solving the problem of optimizing the parameters of the energy storage device at a given maximum energy capacity of 52.6 kWh and power 205 kW and energy consumption 43.2 kWh and power 205 kW

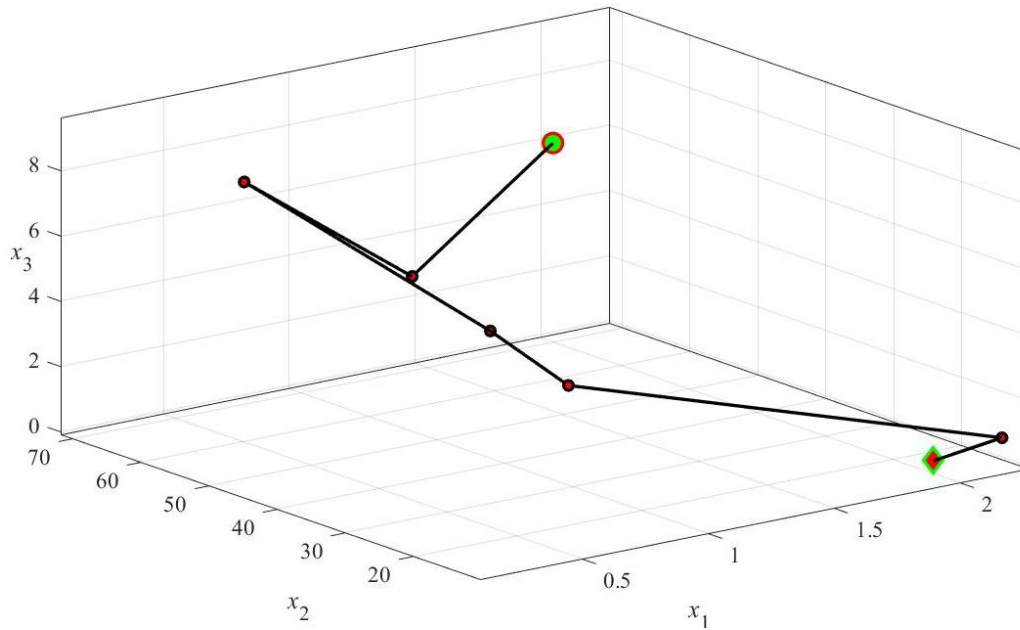


Fig. 2. The progress of solving the problem of optimizing the parameters of the energy storage device at a given maximum energy capacity of 65.6 kWh and power 216 kW and energy consumption 53.8 kWh and power 216 kW

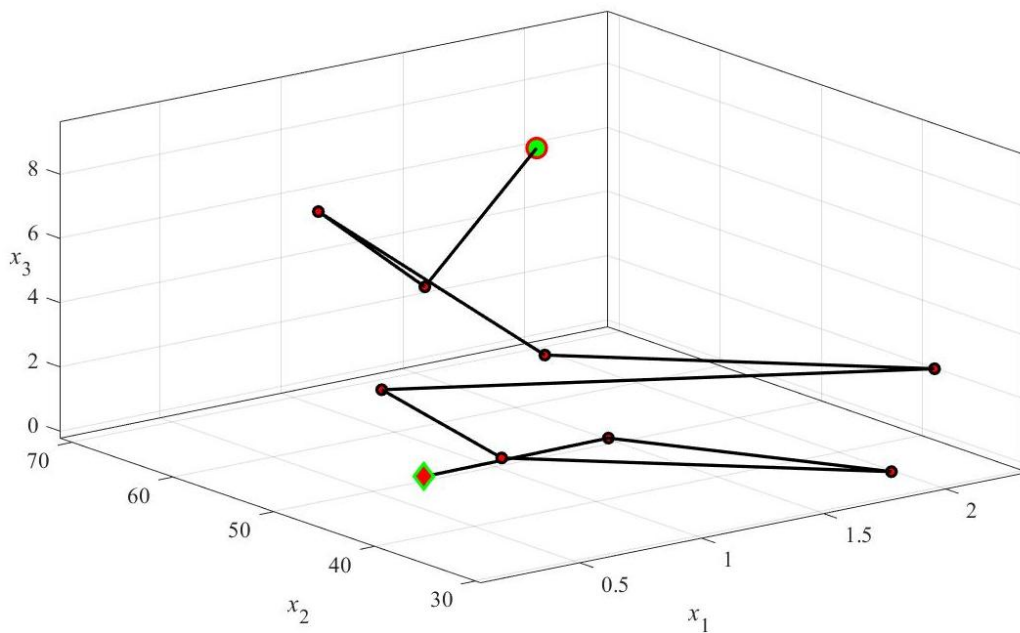


Fig. 3. The progress of solving the problem of optimizing the parameters of the energy storage device at a given maximum energy capacity of 96.4 kWh and power 221 kW and energy intensity 79 kWh and power 221 kW

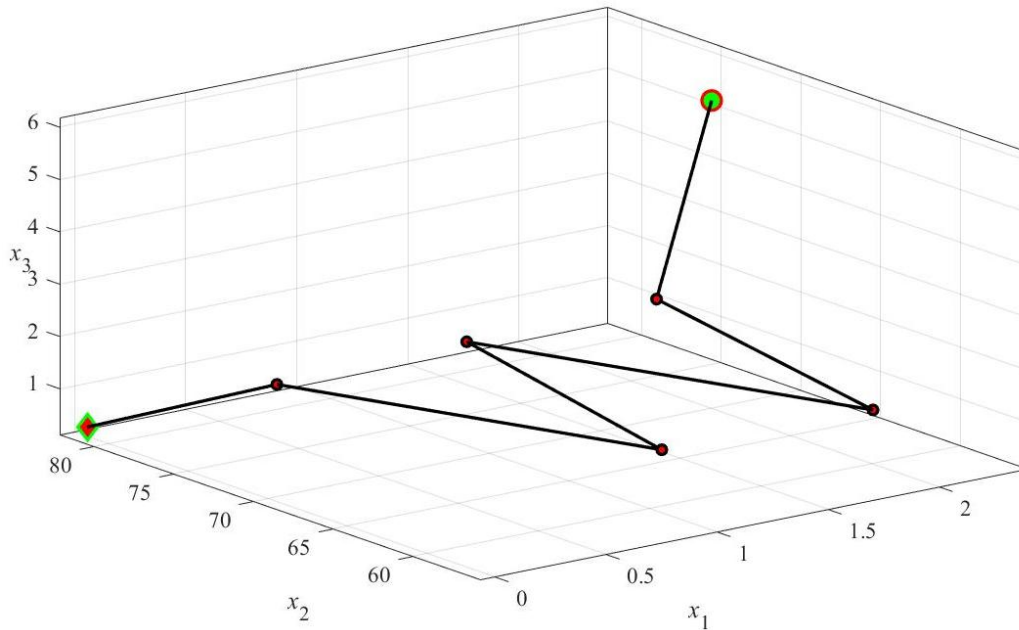


Fig. 4. The progress of solving the problem of optimizing the parameters of the energy storage device at a given maximum energy capacity of 117.6 kWh and power 221 kW and energy consumption

The overall results are presented in Tables 7.

Table 7. Results of solving the problem of finding optimal parameters of the energy storage device when charging an electric bus at terminal stops

Route	W_n	P_n	x_1	x_2	x_3	P	W	M	v	Z
-	kWh	kW	-	-	-	kW	kWh	t	m ³	thousand euros
4	52.6	205	1	28	1	210	74	0.89	0.52	50.91
4	65.6	216	2	15	0	230	71.5	0.883	0.49	52, 49
4	96.4	221	1	47	0	226	107	1.09	0.57	54.44
4	117.6	221	0	81	0	228	146	1.32	0.67	57.83
10	43.2	205	1	28	1	210	74	0.89	0.52	50.91
10	53.8	216	2	15	0	230	71.5	0.883	0.49	52.49
10	79	221	1	47	0	226	107	1.09	0.57	54.44
10	96.4	221	1	47	0	226	107	1.09	0.57	54.44

The assessment of specific indicators of storage tanks is given in Table 8 .

The implementation of an energy storage system for electric bus operation under an opportunity-charging paradigm at equipped terminal stops for routes 4 and 10 reveals that optimal configurations span single-, dual-, and triple-component system architectures. For an economical driving regime on both routes, the optimal configuration is identified as a three-component storage device, comprising 1 branch of LTO cells, 28 branches of LFP cells, and 1 branch of supercapacitors.

Conversely, for intermediate and high-speed driving modes, the optimal solutions shift to dual-component architectures. Specifically, the intermediate mode is best served by a configuration of 2 branches with LTO cells and 15 branches with LFP cells, while the high-speed mode necessitates a system of 1 branch with LTO cells and 47 branches with LFP cells. Under an "obstacle" mode, which simulates demanding traffic conditions, the operational requirements for route 10 can be met by a storage device configured for the "high-speed" regime. However, for route 4, which exhibits a higher energy

demand profile, a more substantial, mono-component storage device based exclusively on LFP elements, comprising 81 branches, is required.

Table 8. Results determination specific indicators of energy storage devices when charging an electric bus at terminal stops

Route	Electric bus driving mode	x_1	x_2	x_3	P_u	W_u	M_u	v_u
-	-	-	-	-	thousand euros /kW	thousand euros / kWh	thousand euros /t	thousand euros /m ³
4	Economical	1	28	1	0.242	0.688	57.202	97.904
4	Intermediate	2	15	0	0.228	0.734	59.445	107.122
4	Fast	1	47	0	0.241	0.509	49.945	95.509
4	Behind obstacles	0	81	0	0.254	0.396	43.811	86.313
10	Economical	1	28	1	0.242	0.688	57.202	97.904
10	Intermediate	2	15	0	0.228	0.734	59.445	107.122
10	Fast	1	47	0	0.241	0.509	49.945	95.509
10	Behind obstacles	1	47	0	0.241	0.509	49.945	95.509

A critical finding of this analysis is that, due to the reduced absolute energy consumption inherent in this operational model, the primary determinant of storage device parameters shifts to power delivery capability. The installed energy capacity for most driving modes consequently represents a significant over-provisioning, with the exception of the "obstacle" mode, where both energy and power are coequally significant constraints. This over-provisioning is quantified as follows: energy capacity exceeds the minimum requirement by 40.7% and 71.2% for routes 4 and 10, respectively, in the economical mode; by 9% and 32.9% in the intermediate mode; and by 11% and 35.4% in the high-speed mode.

The mass of the optimally sized storage devices for this charging strategy is substantially lower - by a factor of 2.4 to 4.14 - compared to the mass of systems designed for depot charging, ranging from 0.89 tonnes to 1.32 tonnes. Correspondingly, the cost of the constituent cells is also significantly reduced, amounting to 50.91 and 57.83 thousand euros, which is 1.84 to 4.41 times lower than the cost of cells required for depot-charging scenarios.

The specific cost metrics for the derived optimal storage device parameters fall within a range of 0.228 to 0.254 thousand euros per kilowatt-hour for specific power, and 0.396 to 0.734 thousand euros per kilowatt-hour for specific energy. This cost structure is directly attributable to the predominant utilization of branches equipped with LFP elements in the final configurations.

Assessment of shortcomings and prospects for the development of the above research. When optimizing the parameters of energy storage devices for electric buses, the main drawback is not taking into account the transient processes of the multi-component energy storage device during the movement of the electric bus along the route. Significant energy flows between components and the rate of energy exchange between cells of different types significantly depend on the type of semiconductor control converter and the modes of movement of the electric bus. Therefore, the main direction of further research may be the determination of the parameters and modes of operation of the multi-component semiconductor converter control system.

Conclusions. When using an energy storage device for an electric bus when charging an electric bus at the final equipped stop on routes 4 and 10, it is also optimal to use a single-, two-component and three-component type of storage device. So, for economical movement on routes 4 and 10, three-component storage devices with 1 branch with LTO cells and 28 branches with LFP cells and 1 branch of supercapacitors are optimal. When moving in intermediate and high-speed modes, two-component

storage devices with the following parameters are optimal: 2 branches with LTO cells and 15 branches with LFP cells and 1 branch with LTO cells and 47 branches with LFP cells, respectively. For the obstacle mode, a storage device operating in the "high-speed" mode is sufficient for route 10, however, for route 4, which requires higher energy consumption, it is necessary to use a mono-component LFP - an element storage device with 81 branches. Due to the reduction in energy consumption requirements, the main factor determining the storage device parameters is power, and the energy consumption for such modes of operation of the electric bus is excessive except for the "obstacle" mode, where both factors are significant. Thus, the energy consumption in the economic mode exceeds the minimum required for 4 and 10 by 40.7% and 71.2%, respectively, for the "Intermediate" mode by 9% and 32.9%, and for the "High-speed" mode by 11% and 35.4%. The mass of the storage device is significantly less (2.4-4.14 times) than the mass of an electric bus when charging at a depot and ranges from 0.89 t to 1.32 t. As for the cost of the cells, their cost is 50.91 and 57.83 thousand euros, which is significantly lower than the cost of cells (1.84 – 4.41 times) when charging an electric bus at a depot.

REFERENCES

1. Kondratyeva, L. Yu., & Ryabov, E. S. (2022). Preliminary analysis of options for building an on-board energy storage system for an electric locomotive. *Theoretical and practical research of young scientists: proceedings of the XVI International Scientific and Practical Conference of Master's and PhD Students* (p. 421). Kharkiv: NTU "KhPI". https://science.kname.edu.ua/images/dok/konferentsii/2025/Tezi%20konferencij%202025/Materiali_KONFERENCIA_2_24_ZOVTNA_2025.pdf. [in Ukrainian]
2. Kondratieva, L., Overianova, L., Tkachenko, V., Riabov, I., & Demydov, O. (2024). Simulation of the operation of the on-board energy storage in the traction system of a quarry locomotive. *Transport Systems and Technologies*, (43), 136–148. <https://doi.org/10.32703/2617-9059-2024-43-11>.
3. Goolak, S., Kondratieva, L., Riabov, I., Keršys, A., & Makaras, R. (2023). Research and optimization of hybrid on-board energy storage system of an electric locomotive for quarry rail transport. *Energies*, 16(7), 3293. <https://doi.org/10.3390/en16073293>.
4. [Qualification work]. (n.d.). *ELARTU Institutional Repository of Ternopil Ivan Puluj National Technical University*. Retrieved from: <https://elartu.tntu.edu.ua/bitstream/lib/43534/2/Кваліфікаційна%20робота.pdf>. [in Ukrainian]
5. Babiy, M. V., Dolynnyi, A. V., & Kostyuk, E. R. (2019). Setting the main tasks of organizing trolleybus transportation. *Proceedings of the VIII International Scientific and Technical Conference of Young Scientists and Students "Actual Problems of Modern Technologies"* (vol. 1, pp. 159–160). Ternopil: TNTU. <http://elartu.tntu.edu.ua/handle/lib/30758>. [in Ukrainian]
6. KP "Electroavtotrans". (n.d.). *Official website*. Retrieved from: <http://eat.if.ua/>. [in Ukrainian]
7. Hnatov, A., Argun, Sch., & Bykova, Ye. (2016). Electric bus on supercapacitors for urban transportation. *Bulletin of the Kharkiv National Automobile and Road University*, (72), 29–34. <https://europub.co.uk/articles/-A-164844>. [in Ukrainian]
8. *Vehicle Emission Standards*. (2016). Retrieved September 3, 2018, from: <https://infrastructure.gov.au/vehicles/environment/emission/index.aspx>.
9. Khaustov, O. (2025). Choosing the type of cells for a multi-component energy storage system for an electric bus that is charged at a depot. *Energy saving. Energy. Energy audit*, 9(212), 41–56. <https://doi.org/10.20998/2313-8890.2025.09.04>. [in Ukrainian].
10. National Commission for State Regulation in the Spheres of Energy and Utilities. (2015, February 26). *On Setting Tariffs for Electricity Sold to the Population* (Resolution of the National Commission for State Regulation in the Spheres of Energy and Utilities No. 220). <https://zakon.rada.gov.ua/laws/show/z0231-15#Text>. [in Ukrainian]
11. Soroka, K. O., & Lychov, D. O. (2017). Increasing the efficiency of electric transport operations through control and optimization of speed regimes. *Bulletin of NTU "KhPI"*, 27(1249), 289–293. [in Ukrainian]
12. Soroka, K. O., & Lychov, D. O. (2015). Meaningful model and equations of electric transport movement. *Bulletin of the Dnipropetrovsk National University of Railway Transport*, 3(57), 97–106. <https://doi.org/10.15802/stp2015/46056>. [in Ukrainian].
13. Yinlong Energy. (n.d.). *Yinlong battery*. Retrieved from: <https://www.yinlong.energy/yinlong-battery#footer>.
14. Enerprof. (n.d.). *Enerpower 26650 LiFePO4 3.2V 3000mAh 10C*. Retrieved from: <https://enerprof.de/en/lifepo4-batteries/lifepo4-battery-cells/lifepo4-battery-cells-26650/36/enerpower-26650-lifepo4-3.2v-3000mah-10c>.
15. Maxwell Technologies. (2021). *New 2.7V 3000F Cell Datasheet*. Retrieved from: https://maxwell.com/wp-content/uploads/2021/09/3003279.2_Final-DS_New-2.7V-3000F-Cell_20210406.pdf.
16. Nikulina, O. M., Severyn, V. P., & Kotsiuba, N. V. (2020). Development of information technology for optimizing the control of complex dynamic systems. *Bulletin of the National Technical University "KhPI". Series: System Analysis, Management and Information Technologies*, 2(4), 63–69. <https://repository.kpi.kharkov.ua/handle/KhPI-Press/50285>. [in Ukrainian].

17. Severyn, V. P., & Nikulina, O. M. (2023). *Methods and algorithms of multidimensional unconditional optimization: a textbook*. Kharkiv: NTU "KhPI". <https://repository.kpi.kharkov.ua/handle/KhPI-Press/67856>. [in Ukrainian].
18. Nikulina, O. M., & Severyn, V. P. (2024). *Numerical methods for modeling and optimization of control of dynamic systems: a textbook*. Kharkiv: NTU "KhPI". <https://repository.kpi.kharkov.ua/handle/KhPI-Press/73689>. [in Ukrainian].
19. Liubarskyi, B., Iakunin, D., Nikonov, O., Liubarskyi, D., & Yeritsyan, B. (2022). Optimizing geometric parameters for the rotor of a traction synchronous reluctance motor assisted by partitioned permanent magnets. *Eastern-European Journal of Enterprise Technologies*, 2(8(116)), 38–44. <https://doi.org/10.15587/1729-4061.2022.254373>.
20. Khaustov, O., & Liubarskyi, B. (2025). Optimization of quasi-steady-state operating modes of synchronous jet motors with permanent magnets for electric buses. *Energy saving. Energy. Energy audit*, 3(206), 16–30. <https://doi.org/10.20998/2313-8890.2025.03.02>. [in Ukrainian].

Олександр Хаустов¹, Борис Любарський²

¹Аспірант, Кафедра електричного транспорту та тепловозобудування, Національний технічний університет «Харківський політехнічний інститут», вул. Кирпичова, 2, м. Харків, Україна, 61002, Україна. ORCID: <https://orcid.org/0009-0001-0363-6173>.

²Професор, Кафедра електричного транспорту та тепловозобудування, Національний технічний університет «Харківський політехнічний інститут», вул. Кирпичова, 2, м. Харків, Україна, 61002, Україна. ORCID: <https://orcid.org/0000-0002-2985-7345>.

Оптимізація параметрів накопичення енергії електробусів, що заряджаються на кінцевих зупинках

Анотація. В роботі розроблено методологію визначення оптимальних параметрів комбінованого накопичувача енергії для електробуса на основі вирішення задачі умовної мінімізації з урахуванням режиму руху, параметрів маршруту, та обмежень за вагою та розмірами при заряджанні накопичувача на кінцевих зупинках маршруту. Практичне значення роботи полягає у визначенні параметрів комбінованих накопичувачів енергії для електробуса на прикладі багатокомпонентного накопичувача енергії. Аналіз результатів дослідження щодо вирішення задачі оптимізації довів, що при економічному русі на маршруті 4 та 10 оптимальними є трикомпонентні накопичувачі з 1 гілкою з LTO-елементами та 28 гілок з LFP – елементами та 1 гілкою суперконденсаторів. При русі у проміжному та швидкісному режимах оптимальними є двокомпонентні накопичувачі з параметрами: 2 гілки з LTO-елементами та 15 гілок з LFP – елементами та 1 гілка з LTO-елементами та 47 гілок з LFP – елементами, відповідно. Для режиму з перешкодами для 10 маршрути достатньо накопичувача, що працює у «швидкісному» режимі, однак для 4 маршруту, що вимагає більшої енергоємності необхідно застосування моно компонентного LFP – елементного накопичувача з 81 гілкою.

Keywords: тяговий привод, накопичувач енергії, електробус, тролейбус, оптимізація параметрів, цільова функція.